Computers and Concrete, *Vol. 24, No. 3* (*2019*) *223-236*
DOI: https://doi.org/10.12989/cac.2019.24.3.223

Simulation of cyclic response of precast concrete beam-column joints

Mahdi Adibi*, Roozbeh Talebkhah[a] and Aliakbar Yahyaabadi[b]

School of Civil Engineering, College of Engineering, University of Bojnord, Iran

(*Received March 7, 2019, Revised June 16, 2019, Accepted June 20, 2019*)

Abstract. Experience of previous earthquakes shows that a considerable portion of concrete precast buildings sustain relatively large damages especially at the beam-column joints where the damages are mostly caused by bar slippage. Precast concrete buildings have a kind of discontinuity in their beam-column joints, so reinforcement details in this area is too important and have a significant effect on the seismic behavior of these structures. In this study, a relatively simple and efficient nonlinear model is proposed to simulate pre- and post-elastic behavior of the joints in usual practice of precast concrete building. In this model, beam and column components are represented by linear elastic elements, dimensions of the joint panel are defined by rigid elements, and effect of slip is taken into account by a nonlinear rotational spring at the end of the beam. The proposed method is validated by experimental results for both internal and external joints. In addition, the seismic behavior of the precast building damaged during Bojnord earthquake 13 May 2017, is investigated by using the proposed model for the beam-column joints. Damage unexpectedly inducing the precast building in the moderate Bojnord earthquake may confirm that bearing capacity of the precast building was underestimated without consideration of joint behavior effect.

Keywords: beam-column joints; precast concrete building; nonlinear modeling

1. Introduction

Precast RC frame system is a method for industrialization of construction. Various communities are using technology and advanced equipment to build housing. The most important features of this structural system are the high quality of construction in a less period of time and possibility of working in poor conditions.

Obtained experiences from previous earthquakes showed significant seismic vulnerability of existing concrete precast buildings (Jaya and Vidjeapriya 2012, Nimse *et al*. 2014, Ozturan *et al*. 2006, Parastesh *et al*. 2014, Yahyaabadi *et al*. 2017). It motivated researchers to develop advanced evaluation methods and upgrade ongoing assessment tools (Allahvirdizadeh and Mohammadi 2016).

Conducted experimental investigations on precast beam-column joints introduced shear and bond deterioration as the most widely observed failure modes. These failures occur by developing deep crack at the intersection of beam and column and/or diagonal cracks in the joint panel which follows by reduction in strength/stiffness and increase in the experienced story drift ratio (Jaya and Vidjeapriya 2012, Jiang *et al*. 2016, Nimse *et al*. 2014, Ozturan *et al*. 2006, Parastesh *et al*. 2014). Such failure prevents adjacent beams to reach their flexural capacity representing by formation of plastic hinge in the beams (Alcocer *et al*. 2002, Cheok and Lew 1993, Choi *et al*. 2013, Jaya and Vidjeapriya 2012, Khaloo and Parastesh 2003, Korkmaz and Tankut 2005, Nimse *et al*. 2014, Nishiyama and Wei 2007, Ozturan *et al*. 2006, Parastesh *et al*. 2014, Rodriguez and Blandón 2005, Shariatmadar and Zamani Beydokhty 2014, Xue and Yang 2010). All aforementioned weaknesses led them to present a poor seismic performance; which causes them to damage severely under earthquakes with much less intensity than expected from modern buildings to withstand. Hence, recognizing their possible failure modes and developing reliable methods to predict their responses received a great attention during recent years.

In addition, it should be noted that a different behavior (from hysteresis, hardening and strength point of view) should be expected from interior joints with respect to exterior ones, because confinement level and reinforcement details of the exterior and interior precast beam-column joints are different (Bahrami and Madhkhan 2017, Rezaei *et al*. 2015, Yekrangnia *et al*. 2016).

Considering aforementioned behaviors, it seems hardly possible for the current assessment methods to predict reliably the seismic response of the concrete precast building. It is evident that these methods should be able to capture not only the local behaviors, including that of the joints, beams, and columns but also should precisely represent the global response.

In this regard, several modeling strategies have been proposed in the literature. Conventionally, beam-column joints are modeled using rigid elements (see Fig. 1(a)). This assumption leads to reasonable outcomes for modern structures subjected to ground motions with low/moderate intensity, but it generally overestimates the stiffness (underestimates experienced lateral displacements) of the existing buildings and misleadingly predicts their failure mechanisms (Hakuto *et al*. 2000, Manfredi *et al*. 2008). Moreover, this method cannot predict shear deformations,

*Corresponding author, Assistant Professor
E-mail: m.adibi@ub.ac.ir, mahdi.adibi@gmail.com
[a]MSc.
[b]Assistant Professor
E-mail: a.yahyaabadi@ub.ac.ir

http://www.techno-press.org/?journal=cac&subpage=8 ISSN: 1598-8198 (Print), 1598-818X (Online)

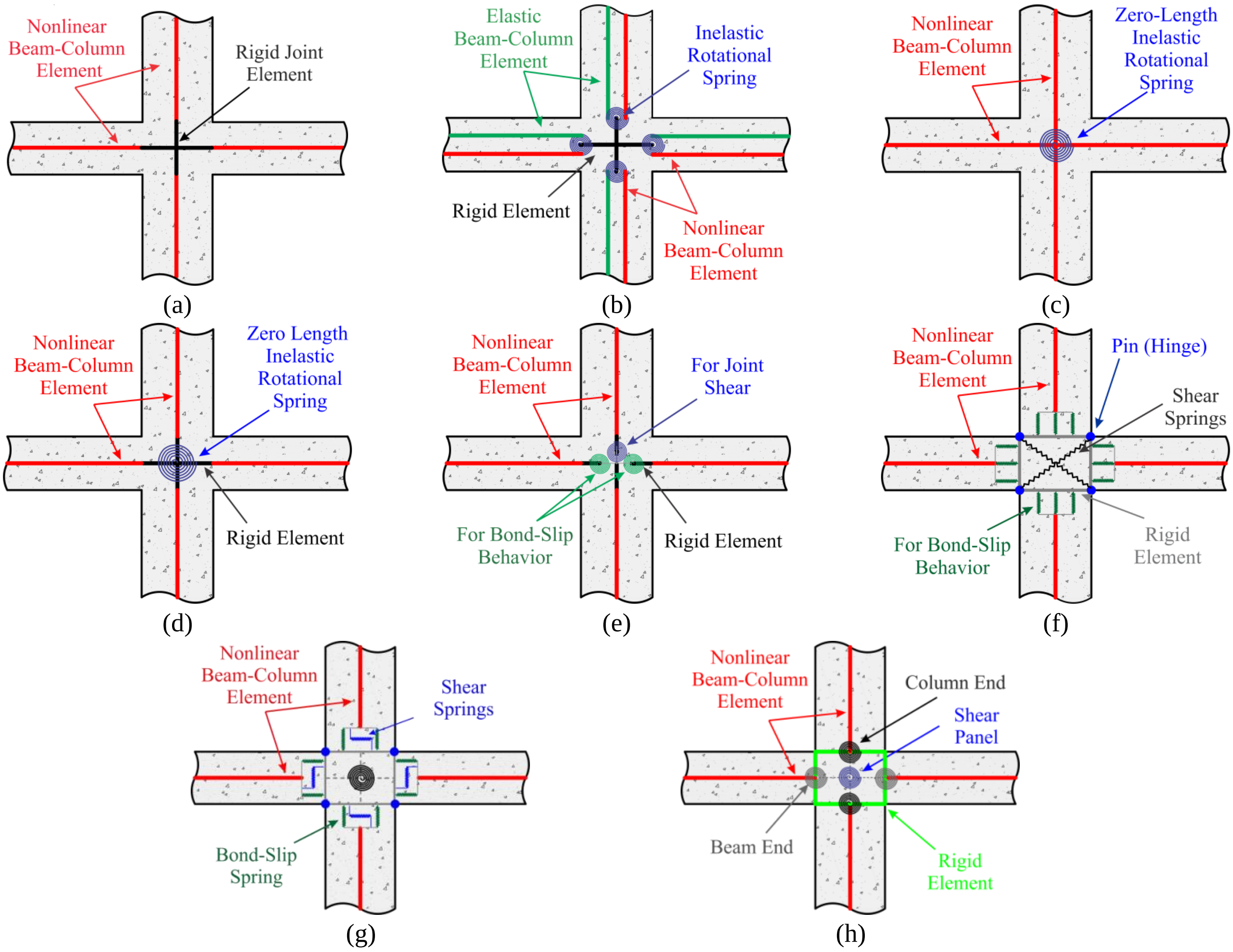

Fig. 1 Different joint modeling approaches (a) conventional rigid joint (b) Otani (1974) (c) El-Metwally and Chen (1988) (d) Alath and Kunnath (1995) (e) Biddah and Ghobarah (1999) (f) Yousef and Ghobarah (2001) (g) Lowels and Altoontash (2003) (h) Altoontash (2004)

diagonal cracking and bond loss (rebar slippage) which was widely observed even in modern buildings under strong earthquakes, and it was shown that have a significant contribution on experienced lateral displacements (Allahvirdizadeh and Gholipour, 2017, Allahvirdizadeh *et al*. 2017, Manfredi *et al.* 2008). This inaccurate consideration of strength and ductility by rigid element approach (Park 2002) led more detailed modeling techniques to be proposed.

Giberson has proposed assigning a nonlinear rotation spring to each end of the beam-column elements. In this method, the linear elastic elements were used for the beams and columns, hence assigned springs represent both nonlinear deformations of beams (flexural) and joint (shear) (Giberson 1969). These linear beam-column elements were later replaced by two parallel elements (which one was for representing linear elastic behavior, and the other one was for post-elastic behavior) by Otani (1974). In this method, the dimension of the joint is again modeled by rigid elements, and rotational springs were introduced into the interface of joint and adjacent components to consider bar slippage (see Fig. 1(b)) (Otani 1974). In the following, the behavior of the joint was decoupled from that of the beam/column by assigning a zero-length element (rotational spring) at its midsection. It is worthwhile to note that some of these methods take into account the dimension of the joint by rigid links, whereas the others continue beam-column elements and directly connect them to the joint spring (Fig. 1(c) and (d)) (El-Metwally and Chen 1988, Alath and Kunnath 1995).

Later, this model was modified by substituting the single spring with a group of springs in series, which can separately consider shear deformations of the joint and bar slippage (Fig. 1(e)) (Biddah and Ghobarah 1999). A relatively same model was proposed by Yousef and Ghobarah, whereas they used diagonal shear springs to connect the hinges at corners of the joint. These hinges were horizontally connected to each other by rigid elements, and bar-slip springs were added at the intersection of each beam/column with the joint (Fig. 1(f)) (Youssef and Ghobarah 2001). The same approach is followed by Lowes and Altoontash, which is schematically depicted in Fig. 1(g) (Lowes and Altoontash 2003). As it is clear, a variety of parameters are required to be defined in each joint zone, which makes its application to be a complicated task. Therefore, a simplified model was developed by Altoontash (2004), which interface springs (consisted of twelve springs for an interior joint) were replaced by four rotational

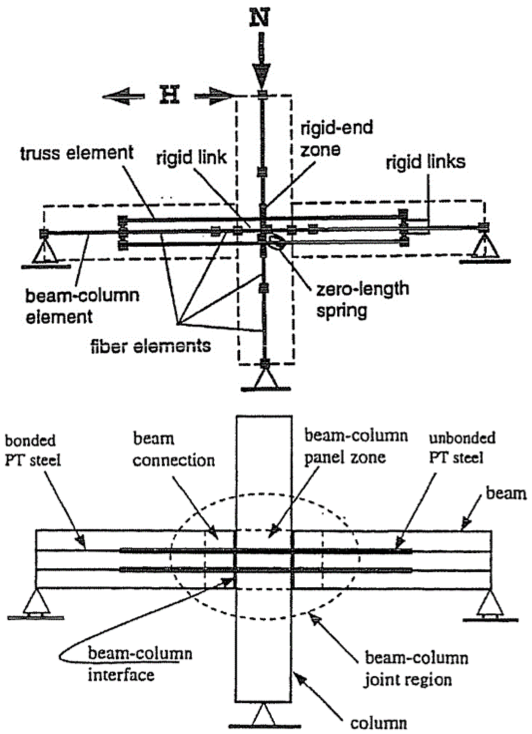

Fig. 2 Fiber model proposed by Pampanin *et al*. for behavior of precast post tensioned beam-column subassembly (Pampanin *et al.* 2001)

(a) Northern side of building

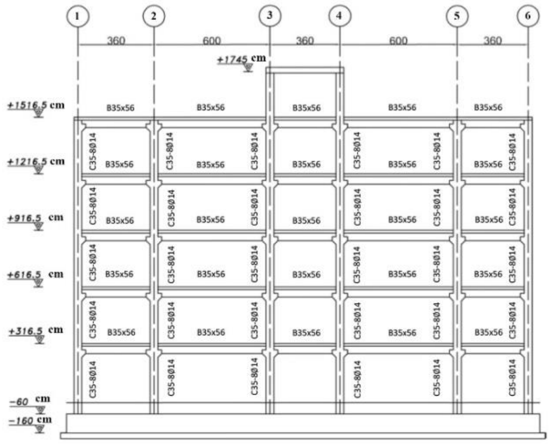

(b) Dimensions of the 2D five storey frame

Fig. 3 Precast Building (Deesman) damaged in Bujnord earthquake of May 13, 2017, Iran

springs (Fig. 1(h)). It is worthwhile to note that in spite of all achieved progresses in consideration of joint behavior on seismic behavior of RC buildings, the discontinuity influence of the beam and column is still not well addressed and understood.

Minor studies have been focused particularly on the seismic response of precast concrete structures. Among which Pampanin *et al*. studied analytical modelling of the seismic behavior of the precast concrete frames designed with ductile connections (Pampanin *et al*. 2001). They propose a fiber model for behavior of precast post tensioned beam-column subassembly (Fig. 2). Most studies on modeling of precast joints are limited by finite element method (Daniel 2006, Dere and Dede 2011, Hawileh *et al*. 2010, Kaya and Arslan 2009, Mostofinejad and Talaeitaba 2006, Wang 2010).

The proposed model in this study is relatively similar to that of Calvi *et al*. (2002) and Alath and Kunnath (1995), (see Fig. 1(d)), i.e., the joint geometry is modeled by rigid elements, and an equivalent rotational spring is added to the midsection. Characteristics of the moment-rotational spring in the model proposed by Pampanin *et al*. are derived by considering the equilibrium between principal tensile stress and shear deformation (Calvi *et al.* 2002), which can be obtained by considering the contraflexure points of adjacent beams/columns at their mid-span and assuming principal tensile stress at the crack initiation point of the joint to be equal to $0.2\sqrt{f_c'}$ and $0.4\sqrt{f_c'}$ respectively for exterior and interior joints. Additionally, a perfectly plastic post-elastic behavior was considered for exterior joints, however, a hardening up to $0.42\sqrt{f_c'}$ principal tensile stress was proposed for interior joints. Regarding the nonlinear behavior of beams and columns, concentrated plasticity approach is employed by assigning rotational springs at their intersections with the joint (Calvi *et al.* 2002). The aforementioned model is valid for the joints which their failure mode includes diagonal shear crack, whereas some other RC subassemblies such as concrete precast joints may fail due to developing cracks at the intersection of the adjacent beam and the joint. Hence, in the current article, an innovative joint model is proposed to capture reliably the post-elastic behavior of such components for both of interior and exterior joints. In this regard, experimental behavior of some precast joint specimens were employed for calibration of the new model. Outcomes of these tests were adopted to propose an empirical rotational spring model. This approach is validated by constructing nonlinear models of the tested specimens in OpenSees software framework (Opensees 2016), which revealed accuracy and reliability of the proposed model. Finally, lateral behavior of a 2D precast frame damaged in Bojnord earthquake of May 13, 2017 was investigated by using the proposed model.

2. Practice of the precast building

The precast concrete building represented in this study, refered to the precast building (Deesman) damaged during Bojnord earthquake in Iran on 13th May 2017 (Fig. 3 and Fig. 4). In this structural system, the frames consist of

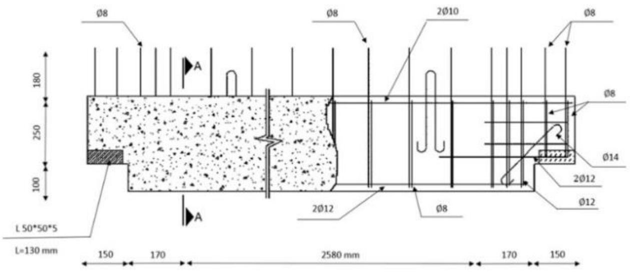

(a)

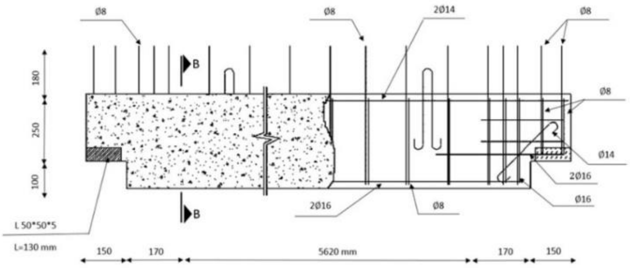

(b)

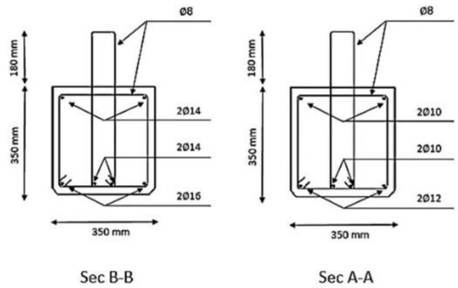

(c)

Fig. 4 (a) Details of the precast beam with length of 3600 mm (b) Details of the precast beam with length of 6000mm (c) Cross sections of the columns and beams in precast beam-column joint

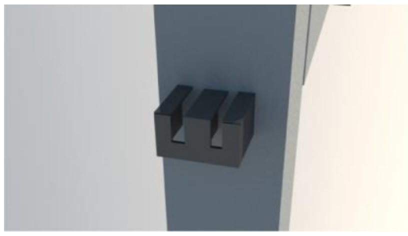

(a) Precast column

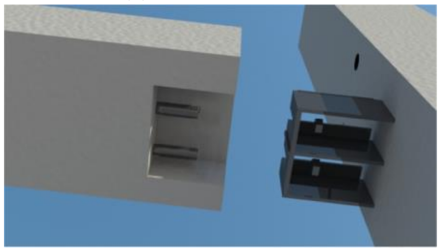

(b) Beam-column connection before installation

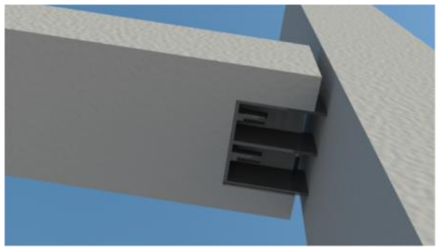

(c) Beam-column connection after installation

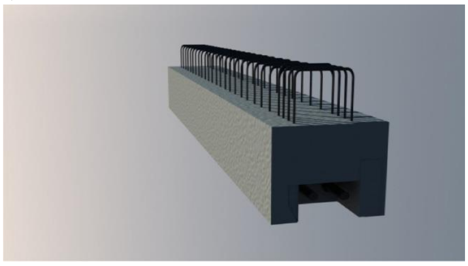

(d) Precast beam

Fig. 5 Detailing of precast beam-column connection (Bahrami and Madhkhan 2017)

precast column with corbel and semi precast beams manufactured by the factory. After placing the beams on the top of the corbel, the connectivity between the beam and corbel created by two shear nuts. Two threaded bars on the top of the beam were passed through the stirrups and two holes in the column, and then empty space of the joint and holes in the column were filled by expandable grout. Represented details of precast beam-column joints are shown in Fig. 5. The compressive strength of the concrete and the yield strength of reinforcing bars were 25 and 400 MPa respectively.

In this study, two sample of precast beam-column connection that are similar to studied precast Building were selected to investigate seismic performance of the precast building. In the following, details of the experimental joint specimens are given.

2.1 The exterior joint Specimen

Bahrami and Madhkhan (2017) studied performance of a 0.6 scale moment resisting precast concrete beam-column connection subjected to cyclic loading by conducting experiments. The prefabricated concrete column was cast with inverted channel steel corbel (inverted E) embedded in the joint core to connect the beam element (Fig. 5(a)). Four vertical bars were welded to the corbel in the panel zone of the joint in precast column to provides adequate shear strength and stability under the installation and prevent the slip of corbel during lateral loading. The steel corbel provided enough bearing area for sitting the reinforced concrete beam. The semi precast concrete beam was placed on the steel corbel embedded in the continuous column with inverted E shape corbel, and bottom longitudinal bars of the beam were tightened between the grooves of the corbel by two nuts (Fig. 5(b) and 5(c)). Top longitudinal bars of the beam were passed through the stirrups of the beam and holes in the column (Fig. 5(d)). The empty space of the connection and two holes in the column were filled with expandable grout. After grouting, the connection was completed by top part of the beam concreting. The properties of tested beam-column connection is shown in Fig. 6. Precast connection was loaded in lateral form

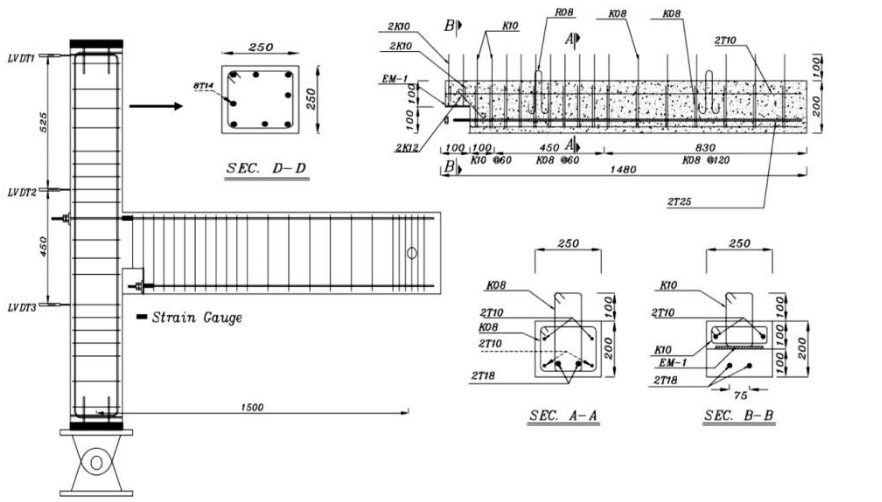

Fig. 6 details of experimental exterior joint specimen (Bahrami and Madhkhan 2017)

Table 1 Mechanical properties of steel and concrete material, and dimensions of the elements in experimental specimens

	compressive strength of the concrete	compressive strength of the grout	yield strength of reinforcing bars		yield strength of steel corbel	
	F'_c (MPa)	F'_c (MPa)	F_y (MPa)	F_u (MPa)	F_y (MPa)	F_u (MPa)
Exterior joint	32	45	452	610	235	390
Interior joint	30	40	400	600	240	370

according to protocol that was taken from ACI T1.1-01 (ACI T1.1-01, Acceptance Criteria for Moment Frames Based on Structural Testing. Reported by ACI Innovation Task Group 1 and Collaborators, 2001) and constant axial force equal to 160 kN on the column (Bahrami and Madhkhan 2017). Summary of the mechanical properties of the steel reinforcement and the compressive strength of the concrete specimens at the age of testing are represented in Table 1.

2.2 The interior joint specimen

Rezaei *et al.* (2015), studied performance of a full scale semi precast interior moment resisting connection subjected to cyclic loading. In the construction of semi-precast beams for interior connection, lower bars and stirrups of the beam are located and then, concrete of the beam casted in place until about two thirds of the beam’s height. At the end of each beam, a steel part (steel corbel) is placed in order to mechanically connect the beam with the dowel bars embedded in the column. After connecting the beam to the column, the top longitudinal bars of the beam (June bars) were passed through the stirrups of the beam and column's holes and embedded in the upper layer of the beams. then The empty space of the connection and holes in column were filled with expandable grout (Rezaei *et al.* 2015). Details of the interior beam-column connection are shown in Fig. 7. Summary of the mechanical properties of the steel reinforcement and the compressive strength of the concrete specimens at the age of testing are represented in Table. 1.

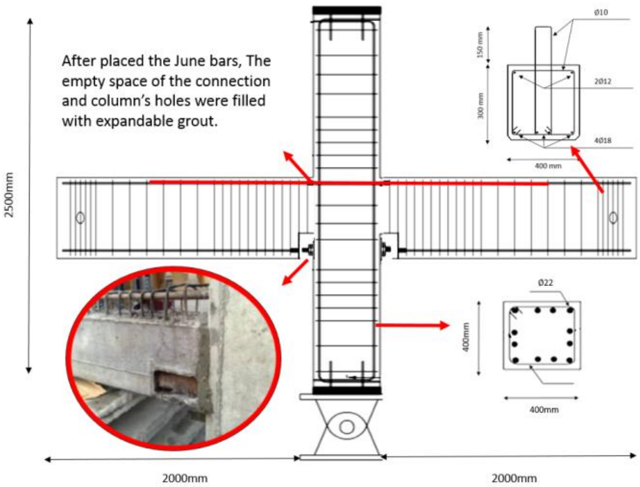

Fig. 7 Details of beam-column connection in the interior joint Specimen (Rezaei *et al.* 2015)

3. Seismic behavior of precast connection

3.1 Behavior of precast connection due to Bojnord earthquake

The represented precast concrete building in this study, refered to the precast building (Deesman) damaged during Bojnord earthquake in Iran on 13th May 2017 (Fig. 3(a) and 3(b)). The magnitude and the PGA of this earthquake was 5.7 M_n and 0.62 g respectively (Iranian Seismological Center, Yahyaabadi *et al.* 2017).

The building designed in 2013, According to current seismic codes and therefore it was not expected any structural damage in the building due to intensity of Bojnord earthquake. But the represented building during the earthquake experienced large lateral displacement and there was some serious damage in the structure that caused the residents dumped the building. After earthquake, a visual inspection of the 5-storey precast building was performed to find out the damage happened in this structure.

As shown in Fig. 8, one of the damage modes of substructure include deep and wide crack exactly on the

Fig. 8 Crack pattern of beam-column joint in Deesman Precast building due to Bojnord earthquake

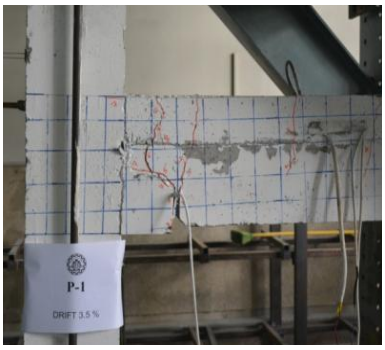

Fig. 10 Crack pattern of the exterior joint specimen at drift ratio of 3.5% (Bahrami and Madhkhan 2017)

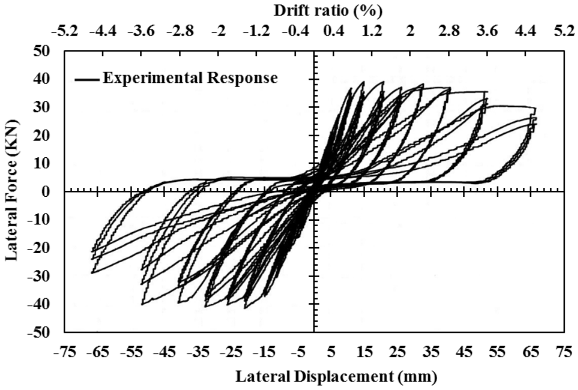

Fig. 9 Lateral load-displacement response of the exterior joint specimen (Bahrami and Madhkhan 2017)

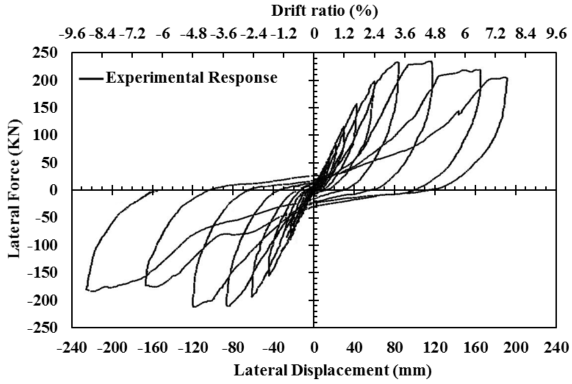

Fig. 11 Lateral load-displacement response of the interior joint specimen (Rezaei *et al.* 2015)

corbel and at the end of the beam. It shows that behavior of precast beam-column joints need to be investigated more (Yahyaabadi *et al.* 2017).

3.2 Behavior of the exterior joint Specimen

In Fig. 9, hysteresis behavior of the experimental exterior joint specimen was represented under cyclic loading. As it was shown in Fig. 10, the substructure tested vertically and the lateral loading was simulated by inducing vertical load at the end of the beam. Pattern of flexural cracking at top and bottom of the beam is different. Initial cracks at top of the beam were appeared at the distance of 1200 mm far from the column face, whereas, at bottom of the beam, cracks were concentrated at the location of precast beam connection to the column and on the corbel. By increasing the load, the flexural cracks at top of the beam were developed along the beam element, but damage to the bottom of the beam concentrated to the cracks on the corbel (Fig. 10). Yielding of the top longitudinal bars of the beam occurred at the drift ratio of 0.81% and Crack widths were opened till 1.25 mm. Maximum load bearing of substructure in forward and backward direction were 39.3 kN and 41.5 kN at the drift ratio of 1.4% and 2.2%, respectively. It shows that moment capacity of the beam that controlled behavior of the substructure were +54 kN.m and 57.1 kN.m in bottom and top of the beam, respectively. The moment capacity of the beam in positive and negative directions was 1.14% and 1.06% of nominal moment capacity of the beam, respectively.

A visual inspection after the test revealed that the slipping of threaded bar was the main reason of the damage inducing to the substructure especially in high level of drift ratio. In addition, lengthening of the beam was seen at the end of the test due to elongation of the bars in cyclic loading. Crushing of concrete was visible at the corners of the beam-column interface. The hysteresis loops of the specimen showed significant pinching and stiffness degradation at drift ratio of 2.75%.

At drift ratio of 4.5%, substructure experienced a reduction of 15% in lateral load capacity, implying the hypothetical failure of the substructure (Bahrami and Madhkhan 2017).

3.3 Behavior of the interior joint Specimen

In Fig. 11, the hysteresis behavior of the experimental interior joint specimen was represented under cyclic loading. In the interior joint, the first flexural cracks occurred at the drift ratio of 0.46% and at the location of the precast beam connection to steel corbel. The cracks pattern of the precast joint at the drift ratio of 6.8% is shown in Fig. 12. According to Fig. 12, main cracks were concentrated at the location of precast beam connection to the column and on the corbel. Also a few diagonal cracks was appeared in the panel zone of the joint. Maximum load bearing of the substructure in forward and backward direction was 210 kN that was corresponded to 1.017% of nominal moment capacity of the beam.

Fig. 12 Crack pattern of the interior joint specimen (Rezaei *et al.* 2015)

4. Proposed model for precast joints

In this section, cyclic responses of the experimental exterior and interior precast beam-column joints were employed to propose a nonlinear model for behavior of precast beam-column joints. As mentioned before, the dominant damage modes in both of exterior and interior precast joints were concentrated at the location of precast beam connection to the column and on the corbel (Fig. 13). In addition, cracking throughout the beams and columns are negligible and diagonal cracking in the joint region is not crucial. Due to the cracking pattern observed in the substructure, it can be assumed that the nonlinear behavior of the section at the end of the beams controls the nonlinear behavior of the substructure. Therefore, a nonlinear rotational spring is considered at the end of the beam at connection to column for introducing the nonlinear behavior of the substructure (Fig. 14). Obviously, characteristics of the spring is largely dependent on the implementation details of the precast joints (Adibi *et al*. 2018). Opensees software framework is used to construct nonlinear models and Displacement-Base Beam-Column element assigned to the beams and columns elements. Panel zone of the joints is modeled by three rigid elements (Opensees 2016). The final parameters assigned to the nonlinear rotational spring can be seen in Fig. 15.

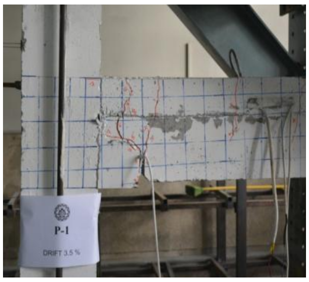

(a)Exterior joint

(b)Interior joint

Fig. 13 Crack patterns of the exterior and interior joint specimens

Nonlinear parameters of the spring have been obtained by calibration of the proposed model by behavior of tested joints specimens. Then, the parameters represented as parametric shapes based on the structural characteristics of precast elements. Elastic deformation of the spring is represented by the elastic rotation of the beam and can be calculated by Eq. (1) .The nonlinear values of the rotational spring have been calculated by experimental behavior of the studied specimens (Adibi *et al.* 2018), which are represented in Table 2.

$$\theta = \frac{M\ L_b}{E\ \ I_b} \tag{1}$$

Where M, L_b, E, I_b, are flexural moment, length, modulus of elasticity and moment inertia of the adjacent beam, respectively.

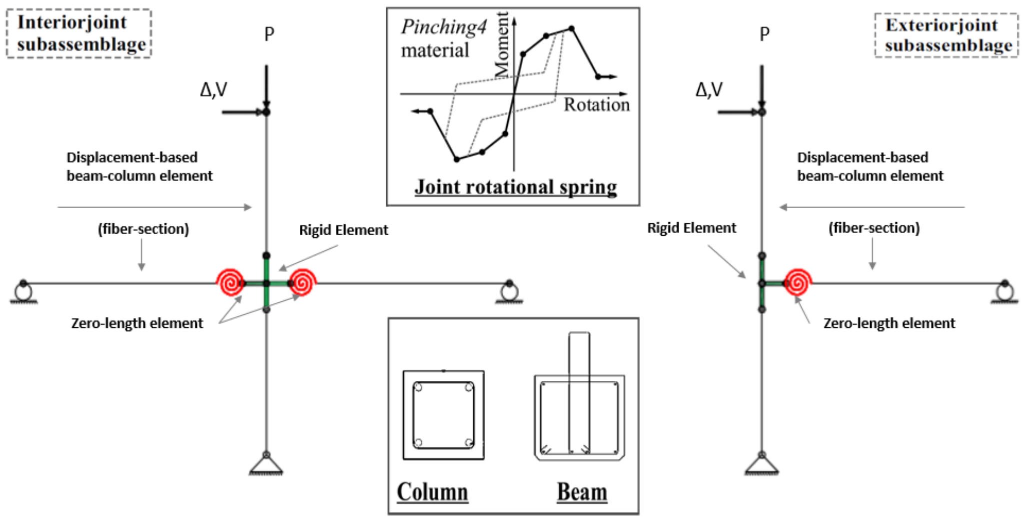

Fig. 14 Proposed model for the exterior and interior precast joint substructures

Table 2 Proposed nonlinear deformations of spring at the precast exterior and interior joint.

a (rad)	*b* (rad)	*c* (rad)	*a'* (rad)	*b'* (rad)	*c'* (rad)
0.001	0.022	0.045	0.001	0.03	0.045

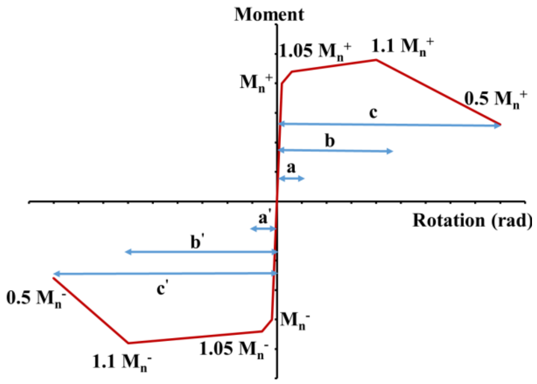

M_n^+ and M_n^- are nominal moment capacity of the beam in positive and negative direction.

(a) Exterior joint

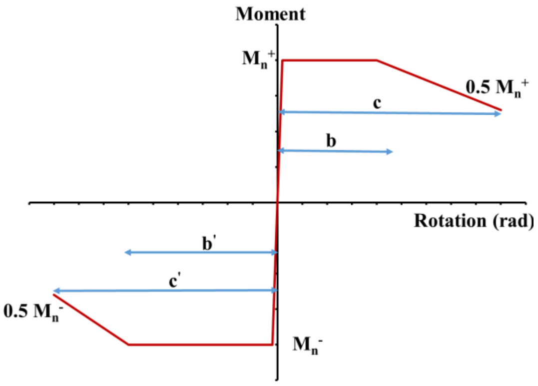

M_n^+ and M_n^- are nominal moment capacity of the beam in positive and negative direction.

(b) Interior joint

Fig. 15 Proposed Nonlinear characteristics of springs at the precast joints

As it was seen in Fig. 14, the differences between the model presented in this study and other researches are: beam and column components modeled by linear elastic elements, dimensions of the joint panel are defined by rigid elements, and effect of slip of the longitudinal bars through the joint is taken into account by a nonlinear rotational spring at the end of the beam.

5. Analytical verification of the proposed model

In this section, comparison between responses of real and simulated beam-column joints are represented. Hysteresis behavior of the exterior and interior beam-column joints reinforced by plain bars are indicated in Fig. 16 (a) and (b). Seismic parameters such as maximum bearing capacity, joint stiffness, energy dissipation and ductility capacity are evaluated for both of real and simulated beam-column joints specimens.

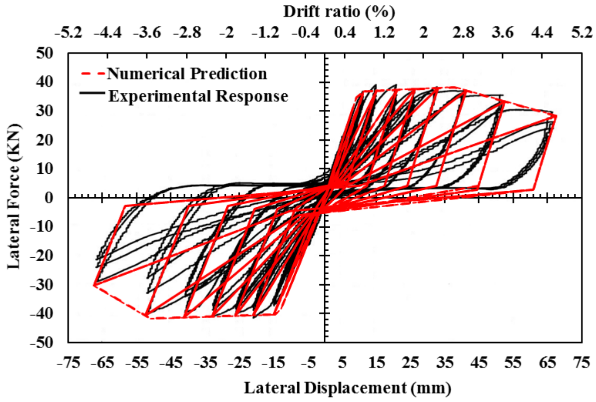

(a) exterior joint

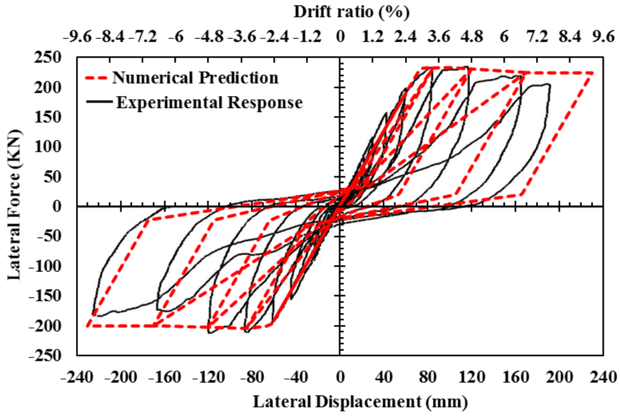

(b) interior joint

Fig. 16 Comparison between simulated Load- Displacement responses with obtained experimental results

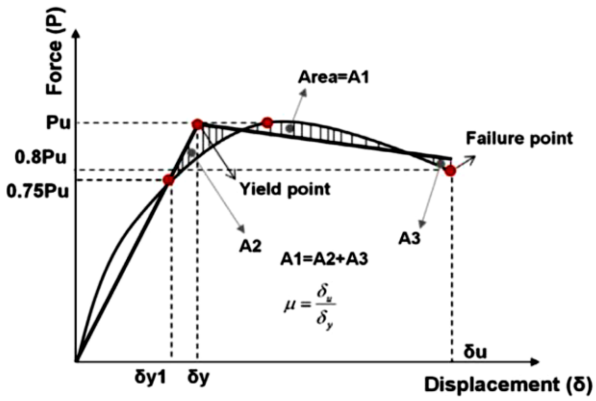

Fig. 17 Characteristic points on force-displacement curve

5.1 Ductility capacity

Ability of structure in inelastic deformation beyond than its elastic state is represented by the ductility factor. Ductility is a necessary parameter in seismic behavior of the substructure. The ductility factor of the substructure is obtained from its idealized bilinear response (see Fig. 17. and Eq. (2)) (Park 1989, Priestley and Park 1987). The ultimate drift, δ_u, is defined as the drift corresponding to either a 20% drop of peak load, the buckling of longitudinal reinforcement, fracturing of longitudinal or transverse reinforcement (Paulay and Priestley 1992).

Table 3 Comparison between simulated ductility factors with obtained experimental results

Beam-Column Exterior Joint		Yield displacement (mm)		Ultimate displacement (mm)		Ductility Factor		Average Ductility Factor
		Pull (+)	Push (-)	Pull (+)	Push (-)	Pull (+)	Push (-)	
Exterior joint	Experimental model	11.36	15.13	60.20	58.14	5.29	3.84	4.56
	Analytical model	10.95	15.27	60.00	61.50	5.47	4.02	4.74
Interior joint	Experimental model	70	55	199.77	234	2.85	4.25	3.55
	Analytical model	75	63.5	229	230	3.05	3.62	3.33

Table 4 Comparison between simulated maximum load bearing capacities and initial stiffness with obtained experimental results

Beam-Column Joint		Maximum bearing capacity (KN)			Initial stiffness (KN/mm)		
		Positive	Negative	Average	Positive	Negative	Average
Exterior joint	experimental model	39.30	41.50	40.4	3.93	2.59	3.26
	Analytical model	38.41	41.91	40.16	3.9	2.86	3.38
Interior joint	experimental model	231	200	215.5	2.89	3.04	2.965
	Analytical model	228.8	213	220.9	2.9	3.16	3.03

5.2 Bearing capacity and stiffness

In Table 4, the maximum load bearing capacities and initial stiffness of precast beam-column joints in the positive and negative directions are represented. The difference between average of maximum bearing capacity of the simulated and real substructure for exterior and interior joint specimens are about 0.6% and 2.5%, respectively. Also the difference between average initial stiffness of simulated and real substructure for the exterior and interior joint are about 3.5% and 2.2%, respectively.

$$\mu = \frac{\delta_u}{\delta y} \tag{2}$$

The calculated ductility capacity for both of real and simulated beam-column joints are reported in Table 3 in both of directions of loading. In this regard, the difference between average ductility factor of simulated and real substructure for the exterior and interior joints are about 4% and 6.6%, respectively. So, it shows that the proposed model has been able to predict the ductility capacity of the substructure almost well.

Cyclic stiffness is defined as the slope of the line that connects the peak positive and negative response during a load cycle as shown in Fig. 18. The result cyclic stiffness of simulated and real subassembly for the exterior and interior joint are shown in Fig. 19 (Saqan 1995).

As shown in Fig. 19, the Secant stiffness degradation in the exterior joint is reduced down to 90% in 4.5% drift ratio, while this reduction in the numerical model corresponds to 89%. Similarly, the proposed model has been able to predict the Secant stiffness degradation of the

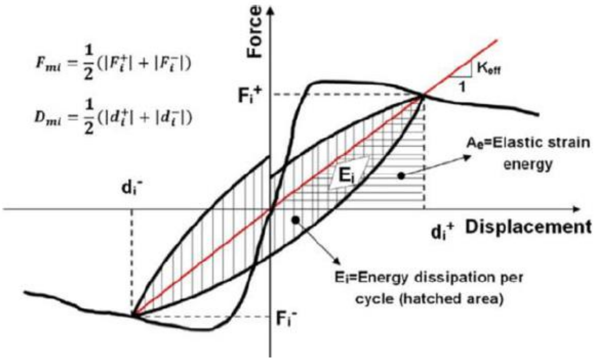

Fig. 18 Definition of Peak to Peak Stiffness (Adibi *et al*. 2017)

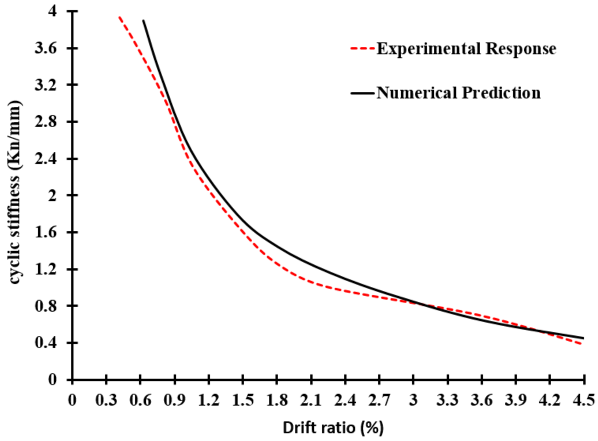

(a) exterior joint

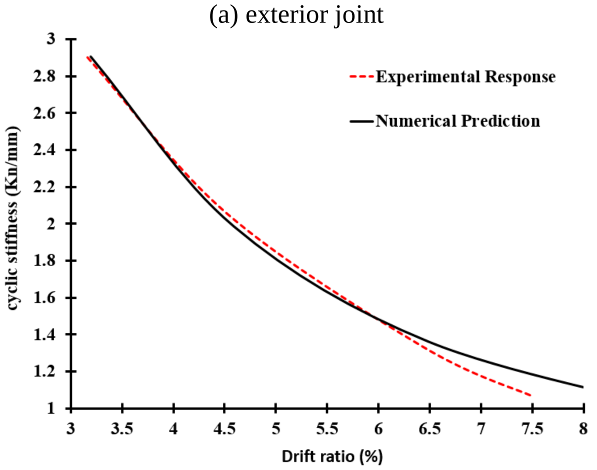

(b) interior joint

Fig. 19 Comparison between simulated cyclic stiffness degradation with obtained experimental results

interior joint specimen until drift ratio of 6.5% relatively well.

5.3 Cumulative energy dissipation

The energy dissipation capacity of a substructure is calculated based on the area under the hysteresis load-deflection curve. Cumulative dissipated energy of the substructures is plotted in Fig. 20 by increasing the drift ratio. As shown in Fig. 20 cumulative energy dissipation of

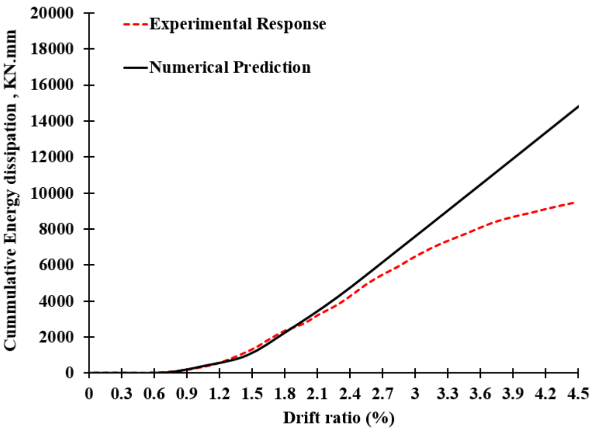

(a) exterior joint

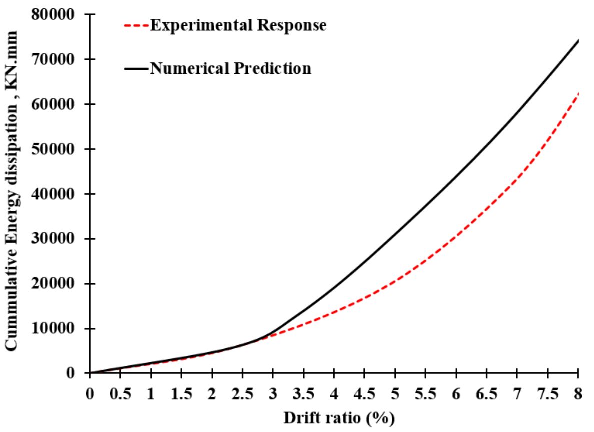

(b) interior joint

Fig. 20 Comparison between simulated Cumulative Energy dissipation with obtained experimental results

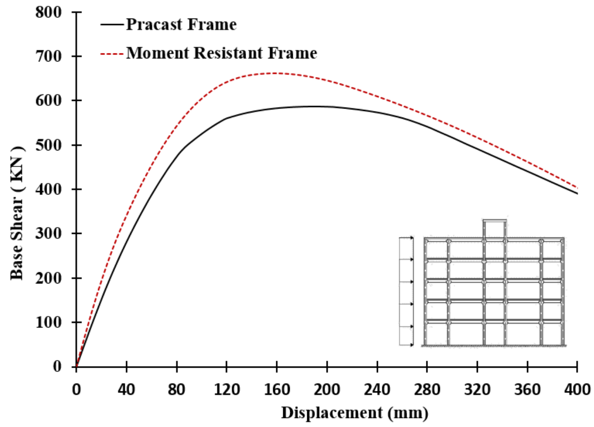

(a) uniform load pattern

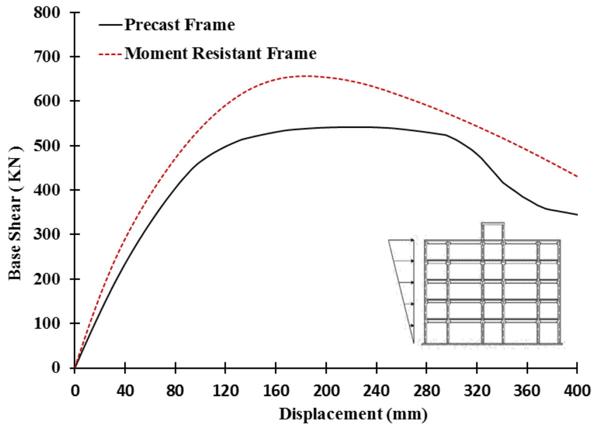

(b) triangular load pattern

Fig. 21 Comparison of nonlinear static analysis results between precast and moment resistant 2D frames

analytical models for the exterior and interior joints have a good confirmation with the test results before drift ratio of 2.7% and 3%, respectively.

With consideration of damage modes in the substructures, the results indicate that the proposed model has been able to predict the energy dissipation of the substructure before reaching to the post yield level.

6. Behavior of a precast 2D frame

In this section, the lateral behavior of a precast 2D frame with consideration of proposed model for behavior of beam-column joint is investigated. The properties of 2D frame is taken from 5-Storey precast concrete building (Deesman) damaged in Bojnord earthquake of May 13, 2017 (Fig. 3). The compressive strength of the concrete and the yield strength of the reinforcing bars in this structure are 25 and 400 MPa, respectively. In this model, the effect of precast joint is considered by the rotational spring located at the beam-column connection zone according to proposed joints model.

In Fig. 21, the results of nonlinear static analysis for 5-Storey precast frame and similar moment resisting frame under the uniform and triangular lateral load pattern are shown. Structural Characteristics of the represented frames such as reinforcement detailing of the beams and columns and compressive strength of the concrete are the same. Seismic parameters of the precast frame such as ductility factor, Maximum bearing capacity, and the initial stiffness, are represented in Table 5 and compared with the similar moment resisting frame. It can be seen that the maximum bearing capacity of the precast frame is less than the moment resisting frame in both of load patterns. As shown in Table 5, Maximum bearing capacity of the precast frame under the triangular and uniform load patterns decrease about 17% and 11%, respectively with respect to the moment resisting frame. According to this table, Initial stiffness of the precast frame under the triangular and uniform load patterns decrease about 25% and 24%,

Table 5 Comparison of seismic parameters between precast and moment resistant 2D frames by different load pattern

Frame type	Ductility factor		Maximum bearing capacity (N)		Initial stiffness (N/mm)	
	load pattern		load pattern		load pattern	
	Triangular	Uniform	Triangular	Uniform	Triangular	Uniform
Moment resisting	4.85	5.34	656040	661306	8459	10275
Precast	3.95	4.8	541840	586864	6369	7833
Variation	-18.6%	-10.1%	-17.4%	-11.3%	-24.7%	-23.8%

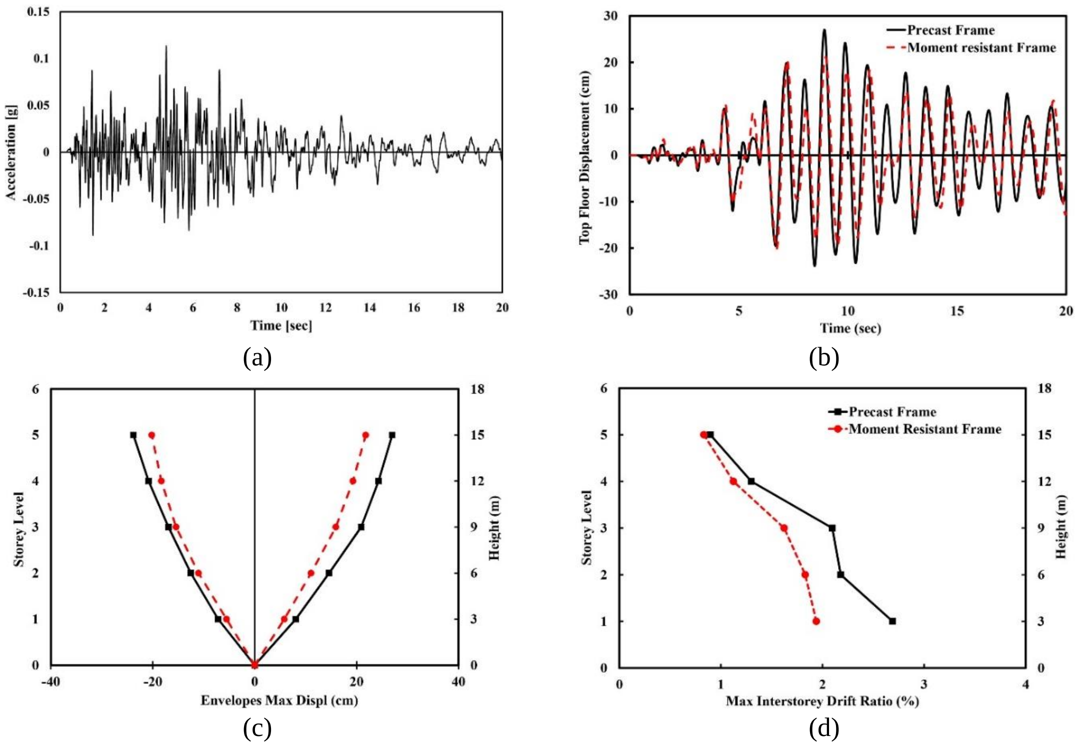

Fig. 22 Comparison of time-history responses of precast building with and without joint modeling under Bojnord earthquake. (a) Acceleration time history of Bojnourd earthquake (b) Top floor displacement (c) Envelope max displacement (d) Max interstorey drift ratio (%)

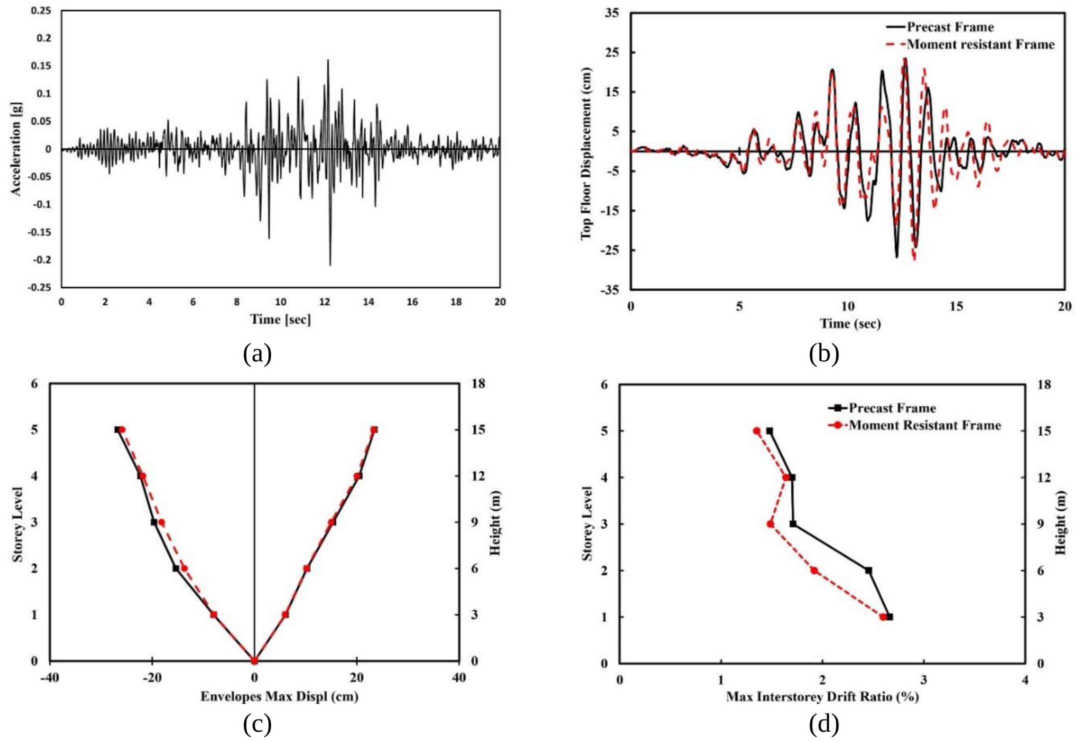

Fig. 23 Comparison of time-history responses of precast building with and without joint modeling under Kocaeli, Turkey earthquake (a) Acceleration time history of Kocaeli, Turkey earthquake (b) Top floor displacement (c) Envelope max displacement (d) Max interstorey drift ratio (%)

respectively with respect to the moment resisting frame. Also ductility factor of the precast frame representing the capacity of plastic deformation of the structure, under the triangular and uniform load patterns decrease about 18% and 10%.

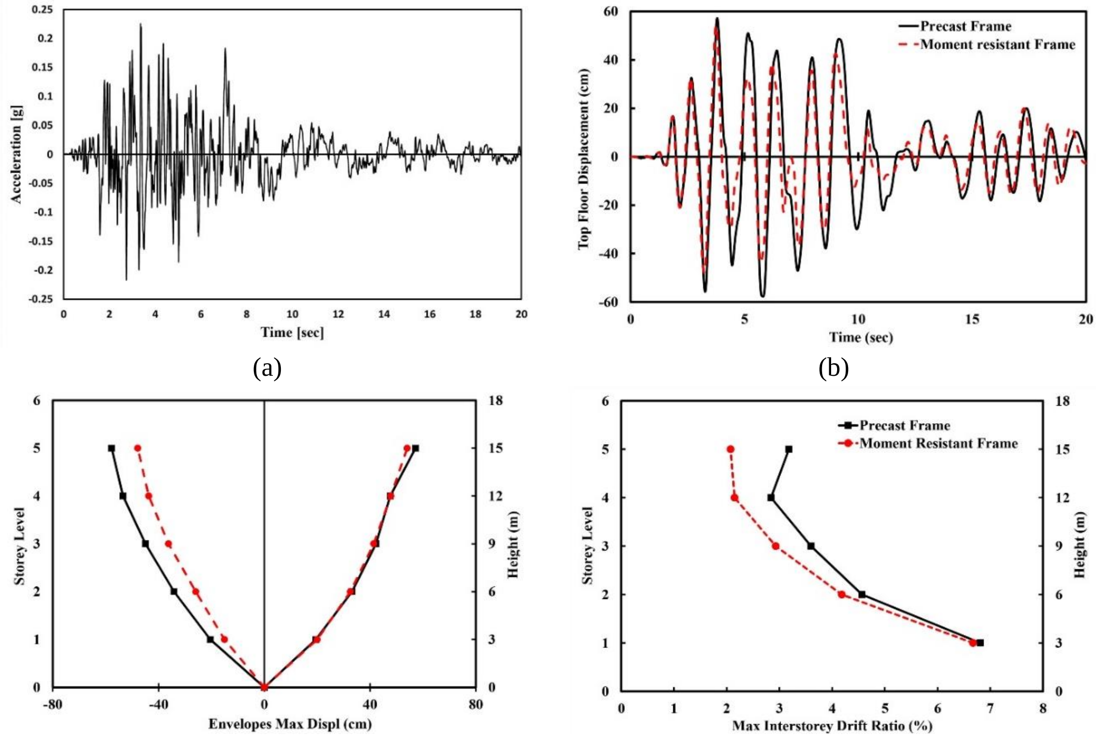

Fig. 24 Comparison of time-history responses of precast building with and without joint modeling under San Fernando earthquake. (a) Acceleration time history of San Fernando earthquake (b) Top floor displacement (c) Envelope max displacement (d) Max interstorey drift ratio (%)

7. Nonlinear dynamic analysis

In this section, the seismic responses of the five-story precast buildings represented in this study, under three different ground motions are shown in Figs. 22-24. The grand motions considered in this study are Bojnord earthquake in Iran, Kocaeli earthquake in Turkey and San Fernando earthquake in US. The proposed model for behavior of the precast joint was used for modeling of the precast building. The effects of precast joint behavior on time-history of floor displacements and maximum interstorey drift ratio of the whole structure are investigated and compared. The results confirm the previous considerations based on preliminary monotonic loading on 2D precast frame. As shown in Figs. 22, 23 and 24, inducing the behavior mechanism of the joint slightly increases the interstorey drift demand and top floor displacement of the building. Observations of the case study and damage inducing to the precast building during Bojnord earthquake confirm that lateral displacement of the building was higher than evaluated by the modeling of the structure without consideration of the precast joint behavior.

8. Conclusions

• The current study was aimed to propose a reliable nonlinear modeling technique for seismic assessment of precast beam-column joints. The proposed model in this research can be used for simulation of the cyclic response of concrete precast beam-column joints were constructed according the usual practice represented in this study. Two tested interior and exterior precast joint specimens by similar details were selected from the literature for calibration of the nonlinear behavior of the proposed model. Finally, the proposed model was employed to evaluate the behavior of the precast building damaged in Bojnord earthquake of May 13, 2017. The obtained outcomes can be summarized as follows:

• Proposed model for simulating the behavior of the precast interior and exterior beam-column joints confirmed the experimental behavior of joint specimens.

◦ The difference between average ductility factor of the simulated and real substructure for the exterior and interior joint specimens are about 4% and 6.6%, respectively.

◦ The difference between average maximum bearing capacity of the simulated and real substructure for the exterior and interior joint specimens are about 1.65% and 3.73%, respectively.

◦ The difference between average Initial stiffness of the simulated and real substructure for the exterior and interior joint specimens are about 3.5% and 2.2%, respectively.

◦ The difference between energy dissipation of the simulated and real substructure for the exterior and interior joint specimens behind the drift ratio of 2.7% and 3% is limited to less than 10%.

• Parameters of seismic behavior of the represented 5-

story precast 2D frame with consideration of the proposed model for behavior of beam-column joint were reduced with regard to the same moment resisting frame.

◦ Maximum bearing capacity of the precast frame under the uniform and triangular loading pattern decreases about 11% and 17% than moment resisting frame, respectively.

◦ Initial stiffness of the precast frame under the uniform and triangular loading pattern decreases about 24% and 25% than moment resisting frame, respectively.

◦ Ductility factor of the precast 2D frame under the uniform and triangular lateral loading pattern decreases about 10% and 18% than moment resisting frame, respectively.

• Nonlinear dynamic analysis of the precast building shows that inducing the behavior mechanism of the joint slightly increases the interstorey drift demand and top floor displacement of the building.

Finally, it seems that according to the precast structures damaged during earthquakes, seismic behavior of precast structures needs more research in some fields such as hysteresis behavior of precast beam-column joints. Results of this study shows that investigation of seismic behavior of precast structures without consideration of the behavior of beam-column joints led to underestimated results.

References

ACI T1.1-01 (2001), Acceptance Criteria for Moment Frames Based on Structural Testing, Reported by ACI Innovation Task Group 1 and Collaborators.

Adibi, M., Marefat, M.S. and Allahvirdizadeh, R. (2018), "Nonlinear modeling of cyclic response of RC beam-column joints reinforced by plain bars", *Bull. Earthq. Eng.*, **16**(11), 1-28. https://doi.org/10.1007/s10518-018-0399-4.

Adibi, M., Marefat, M.S., Arani, K.K. and Zare, H. (2017), "External retrofit of beam-column joints in old fashioned RC structures", *Earthq.. Struct.*, **12**(2), 237-250. https://doi.org/10.12989/eas.2017.12.2.237.

Alcocer, S. M., Carranza, R., Perez-Navarrete, D. and Martinez, R. (2002), "Seismic tests of beam-to-column connections in a precast concrete frame", *PCI J.*, **47**(3), 70-89.

Allahvirdizadeh, R. and Gholipour, Y. (2017), "Reliability evaluation of predicted structural performances using nonlinear static analysis", *Bull. Earthq. Eng.*, **15**(5), 2129-2148. https://doi.org/10.1007/s10518-016-0062-x.

Allahvirdizadeh, R., Khanmohammadi, M. and Marefat, M. (2017), "Probabilistic comparative investigation on introduced performance-based seismic design and assessment criteria", *Eng. Struct.*, **151**, 206-220. https://doi.org/10.1016/j.engstruct.2017.08.029

Allahvirdizadeh, R. and Mohammadi, M.A. (2016), "Upgrading equivalent static method of seismic designs to performance-based procedure", *Earthq.. Struct.*, **10**(4), 849-865. https://doi.org/10.12989/eas.2016.10.4.849.

Altoontash, A. (2004), "Simulation and damage models for performance assessment of reinforced concrete beam-column joints", Stanford university Stanford, California.

Bahrami, S. and Madhkhan, M. (2017), "Experimental performance of a new precast beam to column connection using hidden corbel", *Asia. J. Civil Eng. (BHRC)*, **18**(5), 791-805.

Biddah, A. and Ghobarah, A. (1999), "Modelling of shear deformation and bond slip in reinforced concrete joints", *Struct. Eng. Mech.*, **7**(4), 413-432. https://doi.org/10.12989/sem.1999.7.4.413.

Calvi, G.M., Magenes, G. and Pampanin, S. (2002), "Relevance of beam-column joint damage and collapse in RC frame assessment", *J. Earthq. Eng.*, **6**(spec01), 75-100.

Cheok, G.S. and Lew, H. (1993), "Model precast concrete beam-to-column connections subject to cyclic loading", *PCI J.*, **38**(4), 80-92.

Choi, H.K., Choi, Y.C. and Choi, C.S. (2013), "Development and testing of precast concrete beam-to-column connections", *Eng. Struct.*, **56**, 1820-1835. https://doi.org/10.1016/j.engstruct.2013.07.021.

Daniel, C. (2006), "Finite element analysis of precast prestressed beam-column concrete connection in seismic construction", Master's Thesis, Department of Civil and Environmental Engineering, Chalmers University of Technology.

Dere, Y. and Dede, F.T. (2011), "Nonlinear finite element analysis of an R/C frame under lateral loading", *Math. Comput. Appl.*, **16**(4), 947-958. https://doi.org/10.3390/mca16040947.

El-Metwally, S. and Chen, W. (1988), "Moment-rotation modeling of reinforced concrete beam-column connections", *Struct. J.*, **85**(4), 384-394.

Giberson, M.F. (1969), "Two nonlinear beams with definitions of ductility", *J. Struct. Div.*, **95**, 137-157.

Hakuto, S., Park, R. and Tanaka, H. (2000), "Seismic load tests on interior and exterior beam-column joints with substandard reinforcing details", *Struct. J.*, **97**(1), 11-25.

Hawileh, R., Rahman, A. and Tabatabai, H. (2010), "Nonlinear finite element analysis and modeling of a precast hybrid beam-column connection subjected to cyclic loads", *Appl. Math. Model.*, **34**(9), 2562-2583. https://doi.org/10.1016/j.apm.2009.11.020.

Iranian Seismological Center (Institute of Geophysics, University of Tehran), http://www.irsc.ac.ir.

Jaya, K.P. and Vidjeapriya, R. (2012), "Behaviour of precast beam-column mechanical connections under cyclic loading", *Asia. J. Civil Eng. (Build.Hous.)*, **13**(2), 233-245.

Jiang, H., Chen, Y., Liu, A., Wang, T. and Fang, Z. (2016), "Effect of high-strength concrete on shear behavior of dry joints in precastconcrete segmental bridges", *Steel Compos. Struct.*, **22**(5), 1019-1038. https://doi.org/10.12989/scs.2016.22.5.1019.

Kaya, M. and Arslan, A.S. (2009), "Analytical modeling of post-tensioned precast beam-to-column connections", *Mater. Des.*, **30**(9), 3802-3811. https://doi.org/10.1016/j.matdes.2009.01.033.

Khaloo, A.R. and Parastesh, H. (2003), "Cyclic loading response of simple moment-resisting precast concrete beam-column connection", *Struct. J.*, **100**(4), 440-445.

Korkmaz, H.H. and Tankut, T. (2005), "Performance of a precast concrete beam-to-beam connection subject to reversed cyclic loading", *Eng. Struct.*, **27**(9), 1392-1407. https://doi.org/10.1016/j.engstruct.2005.04.004.

Lowes, L.N. and Altoontash, A. (2003), "Modeling reinforced-concrete beam-column joints subjected to cyclic loading", *J. Struct. Eng.*, **129**(12), 1686-1697. https://doi.org/10.1061/(ASCE)0733-9445(2003)129:12(1686).

Manfredi, G., Verderame, G. and Lignola, G. (2008), "A FEM model for the evaluation of the seismic behavior of internal joints in reinforced concrete frames", *Proceedings of the 14th World Conference on Earthquake Engineering*, Beijing, China.

Mostofinejad, D. and Talaeitaba, S. (2006), "Finite element modeling of RC connections strengthened with FRP laminates", *Iran. J. Sci. Technol., Tran. B, Eng.*, **30**(B1), 21-30.

Nimse, R.B., Joshi, D.D. and Patel, P.V. (2014), "Behavior of wet precast beam column connections under progressive collapse scenario: an experimental study", *Int. J. Adv. Struct. Eng.*

(IJASE), **6**(4), 149-159. https://doi.org/10.1007/s40091-014-0072-3.
Nishiyama, M. and Wei, Y. (2007), "Effect of post-tensioning steel anchorage location on seismic performance of exterior beam-to-column joints for precast, prestressed concrete members", *PCI J.*, **52**(2), 01046620.
Opensees (2016), Open System for Earthquke Engineering Simulation, Pacific Earthquake Engineering Research Center, University of Califonia, Brekely, CA, http://opensees.berkeley.edu/.
Otani, S. (1974), "Inelastic analysis of R/C frame structures", *J. Struct. Div.*, **100**(Proc. Paper 10686).
Ozturan, T., Ozden, S. and Ertas, O. (2006), "Ductile connections in precast concrete moment resisting frames", *Concrete Constr.*, **9**, 11.
Pampanin, S., Priestley, M.N. and Sritharan, S. (2001), "Analytical modelling of the seismic behaviour of precast concrete frames designed with ductile connections", *J. Earthq. Eng.*, **5**(3), 329-367.
Parastesh, H., Hajirasouliha, I. and Ramezani, R. (2014), "A new ductile moment-resisting connection for precast concrete frames in seismic regions: an experimental investigation", *Eng. Struct.*, **70**, 144-157. https://doi.org/10.1016/j.engstruct.2014.04.001.
Park, R. (1989), "Evaluation of ductility of structures and structural assemblages from laboratory testing", *Bull. NZ. Nat. Soc. Earthq. Eng.*, **22**(3), 155-166.
Park, R. (2002), "A summary of results of simulated seismic load tests on reinforced concrete beam-column joints, beams and columns with substandard reinforcing details", *J. Earthq. Eng.*, **6**(2), 147-174.
Paulay, T. and Priestley, M.N. (1992), *Seismic Design of Reinforced Concrete and Masonry Buildings*, John Wiley and Sons, Inc, New York, NY, USA. .
Priestley, M. and Park, R. (1987), "Strength and ductility of concrete bridge columns under seismic loading", *Struct. J.*, **84**(1), 61-76.
Rezaei, F., Madhkhan, M., Nafiyan Dehkordi, V. and Khatibi, J. (2015), "Behavior factor of semi precast RC moment resisting frames with a flexural beam-column connection", *Concrete Res.*, **7**(1), 71-82.
Rodriguez, M.E. and Blandón, J.J. (2005), "Tests on a half-scale two-story seismic-resisting precast concrete building", *PCI J.*, **50**(1), 94-114.
Alath, S. and Kunnath, S.K. (1995), "Modeling inelastic shear deformation in reinforced concrete beam-column joints", *Engineering Mechanics Proceedings of 10th Conference, ASCE*, University of Colorado at Boulder, Boulder, Colorado, 822-825.
Saqan, E.I. (1995), "Evaluation of ductile beam column connections for use in seismic resistant precast frames", PhD thesis, University of Texas, Austin.
Shariatmadar, H. and Zamani Beydokhty, E. (2014), "An investigation of seismic response of precast concrete beam to column connections: experimental study", *Asia. J. Civil Eng.-Build. Hous.*, **15**(1), 41-59.
Xue, W. and Yang, X. (2010), "Seismic tests of precast concrete, moment-resisting frames and connections", *PCI J.*, **55**(3), 102-121.
Yahyaabadi, A., Adibi, M. and bakavoli, M.K. (2017). *Analytical Assessment of Bojnord Earthquake on May 2017*, Bojnord University. (in Persian)
Yekrangnia, M., Taheri, A. and Zahrai, S.M. (2016), "Experimental and numerical evaluation of proposed precast concrete connections", *Struct. Concrete,* **17**(6), 959-971.
Ying Wang, Y.X. (2010), "Nonlinear finite element analysis of the steel concrete composite beam to concretefilled steel tubular column joints", *Int. J. Nonlin. Sci.*, **9**(3), 341-348.
Youssef, M. and Ghobarah, A. (2001), "Modelling of RC beam-column joints and structural walls", *J. Earthq. Eng.*, **5**(1), 93-111.

CC